

Fermi surface arcs and the infrared conductivity of underdoped $\text{YBa}_2\text{Cu}_3\text{O}_{6.50}$

This article has been downloaded from IOPscience. Please scroll down to see the full text article.

2008 EPL 82 27002

(<http://iopscience.iop.org/0295-5075/82/2/27002>)

View [the table of contents for this issue](#), or go to the [journal homepage](#) for more

Download details:

IP Address: 38.107.179.211

The article was downloaded on 22/02/2012 at 05:45

Please note that [terms and conditions apply](#).

Fermi surface arcs and the infrared conductivity of underdoped $\text{YBa}_2\text{Cu}_3\text{O}_{6.50}$

J. HWANG^{1(a)}, J. P. CARBOTTE^{1,2} and T. TIMUSK^{1,2}

¹ *Department of Physics and Astronomy, McMaster University - Hamilton, Ontario L8S 4M1, Canada*

² *The Canadian Institute for Advanced Research - Toronto, Ontario M5G 1Z8, Canada*

received 22 January 2008; accepted 21 February 2008
published online 26 March 2008

PACS 74.72.-h – Cuprate superconductors (high- T_c and insulating parent compounds)
PACS 74.25.Gz – Optical properties
PACS 74.72.Bk – Y-based cuprates

Abstract – We reanalyze the data on the in-plane far infrared conductivity of underdoped orthoII $\text{YBa}_2\text{Cu}_3\text{O}_{6.50}$ ($\text{YBCO}_{6.50}$) in terms of a model in which a pseudogap opens on part of the Fermi surface with the remaining ungapped piece proportional to the temperature. The motivation for our model comes from recent angle-resolved photoemission spectroscopy data in underdoped $\text{Bi}_2\text{Sr}_2\text{CaCu}_2\text{O}_{8+\delta}$ (Bi-2212), which have revealed the existence of arcs on the Fermi surface. We find the optical data to be consistent with arc formation. In addition we find some evidence that the electronic states lost below the pseudogap energy Δ_{pg} are recovered in the energy region immediately above it at least for temperatures near T_c .

Copyright © EPLA, 2008

In going from the overdoped side of the cuprate phase diagram to the underdoped side, a new phenomenon known generally as the formation of a pseudogap is seen [1]. The pseudogap manifests itself in many properties and generally has the signature of a decrease in the electronic density of state (DOS) around the Fermi energy. There is no consensus as to its exact microscopic origin. Some observations are consistent with a preformed pair model [2] with the pseudogap associated with the binding energy of the pairs at the pseudogap temperature T^* and the superconducting temperature T_c the point at which phases lock in and long range order results. Another influential model is a possible competing order such as d -density [3–8] wave which set in at T^* and coexists with the superconducting order parameter below T_c . In this model it may be reasonable to expect two distinct gap scales and some recent data [9,10] have pointed to this possibility.

In the absence of consensus on microscopic origin, phenomenological models have played an important role in understanding and correlating data. An example is the specific-heat data [11,12]. The observed trend from overdoped to underdoped can be understood [11,12] over several families of cuprates by simply introducing a gap

Δ_{pg} in the DOS which obeys a mean-field temperature dependence. More recently, analysis of angle-resolved photoemission spectroscopy (ARPES) data have given a more detailed picture [13] of pseudogap formation on the Fermi surface as a function of temperature. A finite pseudogap first opens at T^* but forms only in a region around the antinodal direction leaving an ungapped Fermi surface arc around the nodal direction of length proportional to the reduced temperature $t = T/T^*$. Here we confine our attention to the normal-state region (above T_c) and study how the formation of Fermi surface arcs modifies optical properties.

Optical-conductivity measurements have given a wealth of information on electron dynamics in the cuprates. While early on the pseudogap was seen clearly as a real gap in the real part of the c -axis [14,15] optical conductivity, its signature in the ab -plane data was less clear and largely confined to a general observation that the optical scattering rate seem to show an additional decrease with decreasing temperature at low frequency as compared with overdoped samples [16]. Only recently has the situation been further clarified when the real part of the optical self-energy was analyzed in more detail [17]. Underdoped samples show a characteristic evolution with decreasing temperature quite distinct from the overdoped case [18–20]. A hat-like peak structure develops at an energy of the order of the pseudogap energy, clearly

^(a) Present address: Department of Physics, University of Florida - Gainesville FL 32611, USA; e-mail: jhwang@phys.ufl.edu

seen above a smooth structureless background. It was recognized that this easily identified [17] feature could be understood in a simple DOS model with a gap below Δ_{pg} and the missing states piled up in the energy region just above the pseudogap which we will refer to here as the recovery region. These modification of the DOS show up very directly in the real and imaginary parts of the optical self-energy $\Sigma^{op}(\omega)$ [21–24].

Consider coupling to a single Einstein mode of energy ω_E . Without a pseudogap (constant electronic DOS) the optical scattering rate $1/\tau^{op}(\omega)$ will be zero till $\omega = \omega_E$ after which it rises from zero according to the law $(\omega - \omega_E)/\omega$ [25]. With a pseudogap it will be zero till $\omega = \omega_E + \Delta_{pg}$ and rise after this according to $(\omega - \omega_E - \Delta_{pg})/\omega$ [20]. On the other hand, if a recovery region is included above $\omega = \Delta_{pg}$ to conserve electronic states, there will be additional scattering in the recovery region due to the extra available states. This will make $1/\tau^{op}(\omega)$ rise more rapidly than it would have without the extra states. This rapid rise in $1/\tau^{op}(\omega)$ translates into the formation of a logarithmic-like structure in Kramers-Kronig transform. Monitoring the growth of this structure in the real part of the optical self-energy $\Sigma_1^{op}(\omega)$ gives us a means to trace pseudogap formation as does the steepness of $1/\tau^{op}(\omega)$ above the energy of the gap plus boson.

There have been many studies of the boson spectra of the cuprates as revealed by tunneling [26], ARPES [27] and optics [20,28–33] in which a spectral density function $I^2\chi(\omega)$ is recovered, where I is a coupling constant between electrons and a boson and $\chi(\omega)$ is the bosonic spectral density. For optimally and overdoped cases, coupling to the sharp resonance at an energy corresponding to the spin-1 collective mode measured in neutron scattering is seen. This resonance starts to exist above T_c in the underdoped case and its intensity (area under the peak) increases with decreasing temperature. For the specific case of orthoII YBCO_{6.50} this has been studied by Hwang *et al.* [20].

In this paper we reanalyze the data on orthoII YBCO_{6.50} allowing for the opening of a pseudogap which covers more of the Fermi surface, as the temperature is lowered below T^* . We ask whether or not the data is consistent with a linear decrease in the length of the remaining arcs as a function of the reduced temperature $t = T/T^*$ as it is seen in the ARPES data in underdoped Bi-2212 [13]. Our analysis of the optical data proceeds through the optical scattering rate $1/\tau^{op}(T, \omega)$. For a system with an energy-dependent self-consistent electronic density of state $N(\omega)$ which is related to the imaginary part of the Green's function $G(\mathbf{k}, \omega)$ by $N(\omega) = 1/\pi \sum_{\mathbf{k}} [-\text{Im}G(\mathbf{k}, \omega)]$ the optical scattering rate can be written approximately [22] as

$$1/\tau^{op}(T, \omega) = \frac{2\pi}{\omega} \int_0^\infty d\Omega I^2\chi(\Omega) \int_{-\infty}^\infty d\epsilon \tilde{N}(\epsilon - \Omega) \times [n(\Omega) + f(\Omega - \epsilon)][f(\epsilon - \omega) - f(\epsilon + \omega)]. \quad (1)$$

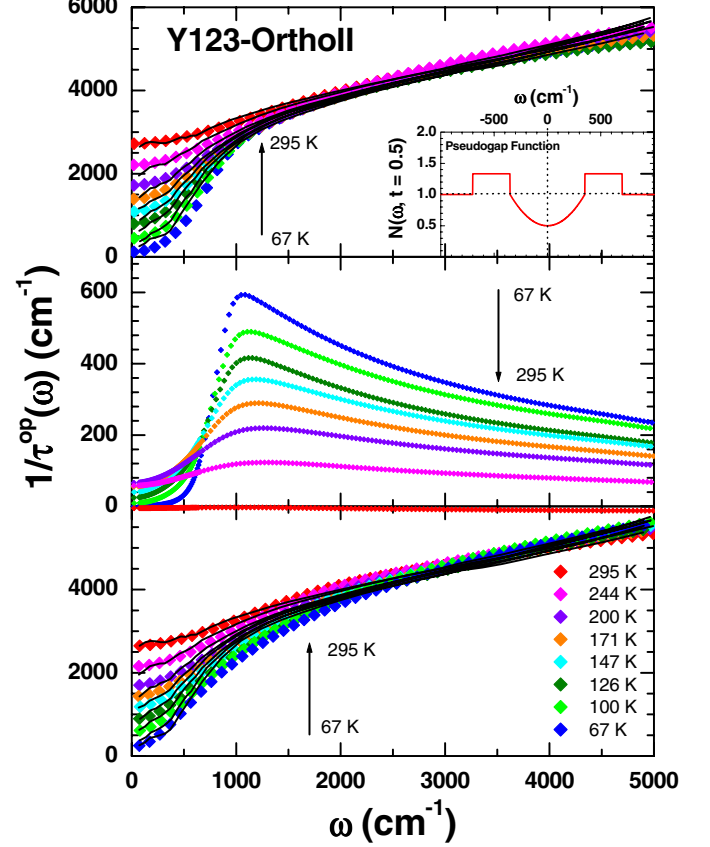


Fig. 1: (Color online) Top frame: optical scattering rate $1/\tau^{op}(\omega)$ in cm^{-1} as a function of ω also in cm^{-1} for the eight temperatures shown (normal state). The heavy solid squares are fits to the data (solid lines). The inset shows the frequency dependence of $\tilde{N}(\omega, t)$ for $t = 0.5$, with quadratic frequency dependence below Δ_{pg} and a constant one above it for $\omega \in (\Delta_{pg}, 2\Delta_{pg})$. Electronic states are conserved. Bottom frame: same as top but previous fit to the data obtained in ref. [20] without including a recovery region above the pseudogap energy which is chosen to conserve state. Middle frame: difference between top frame and scattering rates obtained when the recovery region is excluded, keeping other parameters the same (as top frame fits).

Here $n(\Omega) = 1/[e^{\beta\Omega} - 1]$ is the Bose-Einstein thermal distribution, $f(\epsilon) = 1/[e^{\beta(\mu - \epsilon)} + 1]$ the Fermi-Dirac with β the inverse temperature and μ the chemical potential, and $I^2\chi(\omega)$ the electron-boson spectral density. In eq. (1) $\tilde{N}(\epsilon)$ is the symmetrized electronic density of states $[N(\epsilon) + N(-\epsilon)]/2$. Equation (1) reduces properly to that of Shulga *et al.* [34] in the limit of a constant density of states. It further corresponds to the formula of Allen [35] at zero temperature. The data for $1/\tau^{op}(T, \omega)$ at eight temperatures in the normal state of orthoII YBCO_{6.50} are reproduced [20] in fig. 1 (top and bottom frames) as (dark) solid lines. In all cases the data is fit (solid diamonds of different colors as indicated in the figure) with an electron-boson spectral density $I^2\chi(\omega)$ consisting of a broad Millis-Monien-Pines (MMP) background [36] of

the form $I_0\omega/(\omega^2 + \omega_{sf}^2)$, where I_0 is a coupling between spin fluctuation and charge carriers and ω_{sf} is a typical spin fluctuation energy. In addition a sharp resonance peak modelled by $I_p/[\sqrt{2\pi}(d/2.35)]e^{-(\omega-\omega_p)^2/[2(d/2.35)^2]}$ (where I_p is the area under the peak, ω_p is its center frequency, and d is its width) is included and its position in energy fixed at 31 meV chosen to agree with the energy of the measured spin-1 resonance of inelastic neutron scattering [37]. In addition a pseudogap is included with $\Delta_{pg} = 350 \text{ cm}^{-1}$ fixed from our previous analysis [20] and assumed temperature independent. The length of the remaining ungapped arc is modelled through the self-consistent DOS $\tilde{N}(\omega)$ which we take to be equal to $\tilde{N}(0) + (1 - \tilde{N}(0))(\omega/\Delta_{ps})^2$ for $\omega \leq \Delta_{pg}$ and $2(1 - \tilde{N}(0))/3$ for $\omega \in (\Delta_{pg}, 2\Delta_{pg})$ and 1 beyond this. The value of $\tilde{N}(0)$ is temperature dependent and assumed to be proportional to the reduced temperature $t = T/T^*$. This agrees with the idea that the arc closes linearly in reduced temperature as T is lowered below the pseudogap temperature T^* . Further the lost states below $\omega = \Delta_{pg}$ due to the opening of the pseudogap are taken to reappear above Δ_{pg} in the interval up to $2\Delta_{pg}$. The fitting parameters to the data are area under the resonance peak (I_p) and the background (I_0).

The fits obtained are seen in the top frame of fig. 1 and are seen to be excellent. They are better than the earlier fits obtained in ref. [20] where a pseudogap was included but without arcs and recovery region. These fits are reproduced in the lower frame and are clearly not as good. In particular, in the region around $\omega = 1000 \text{ cm}^{-1}$ the new fits capture the narrow range of variation with temperature observed in the data. This effect is a direct consequence of the temperature dependence assumed for the DOS which itself reflects the temperature dependence of the Fermi surface arcs. When the arcs become smaller with reducing normalized temperature $t = T/T^*$ more states are lost in the pseudogap region as a result of a reduction in the value of $\tilde{N}(\omega)$. But in our model for $\tilde{N}(\omega)$ which is shown in the inset of the upper frame of fig. 1, it is assumed that the lost states are to be found in the region between Δ_{pg} and $2\Delta_{pg}$ so as to respect conservation of states in the electronic DOS. The existence of this recovery region directly leads to more scattering *i.e.* an increase in $1/\tau^{op}(\omega)$ in this energy range than would be the case if no recovery occurred, *i.e.* $\tilde{N}(\omega)$ was equal to its background value of 1. This effect pushes up the $1/\tau^{op}(\omega)$ curves more at low temperatures than at high temperature where the amount of extra states due to recovery is reduced and finally vanishes in our model at the pseudogap temperature $T = T^*$. It is therefore through the effect on $1/\tau^{op}(T, \omega)$ of the recovery region that we see in optics the arcs and their temperature dependence. The arcs have their greatest effects at low temperature as can be seen in the middle frame of fig. 1 where we show the contribution to the optical scattering rate due to the recovery states in $\tilde{N}(\omega)$ above Δ_{pg} . At high temperatures this contribution vanishes as $\tilde{N}(\omega)$ becomes equal to 1

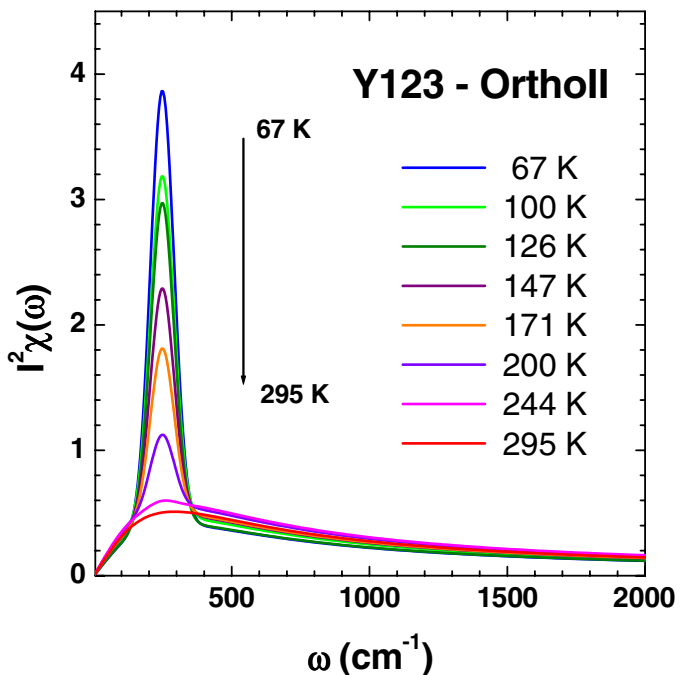


Fig. 2: (Color online) Model electron-boson spectral density $I^2\chi(\omega)$ at various temperatures, obtained from our fits to the scattering rate data assuming an optical resonance peak at 31 meV superimposed on an MMP background.

everywhere. We note that, with increasing T away from T_c , the effect of the recovery region in $1/\tau^{op}(T, \omega)$ becomes small and we cease to be able to extract from the data any quantitative information on the arcs and on the recovery region above it.

In fig. 2 we show the results of our fits for the electron-boson spectral function $I^2\chi(\omega)$ as a function of frequency and temperature. At each temperature the background was allowed to vary as was the area under the resonance peak fixed at an energy of 31 meV [37]. We see that the peak disappears with increasing temperature and at 250 K and above only the background remains. Relative to the peak, the temperature dependence of the background is small.

In fig. 3 we show results for the area under the peak as a function of temperature above the superconducting $T_c = 59 \text{ K}$, *i.e.* in the normal state. The points are denoted by (blue) solid diamond, they are also compared with our previous results from optics (green) open hexagon [20] and with neutron results (purple) solid pentagon [37]. It is seen that the fit to the neutron data has improved as compared to our previous optically derived estimates.

Data on the optical scattering rate in orthoII $\text{YBCO}_{6.50}$ show clear evidence for the formation of a pseudogap which opens at T^* (the pseudogap temperature). We have used a model of the pseudogap with Fermi arcs with linear variation in reduced temperature $t = T/T^*$ as suggested in ARPES experiments on underdoped Bi-2212. The fraction of the Fermi surface which remains ungapped provides a finite but reduced value for the self-consistent density of

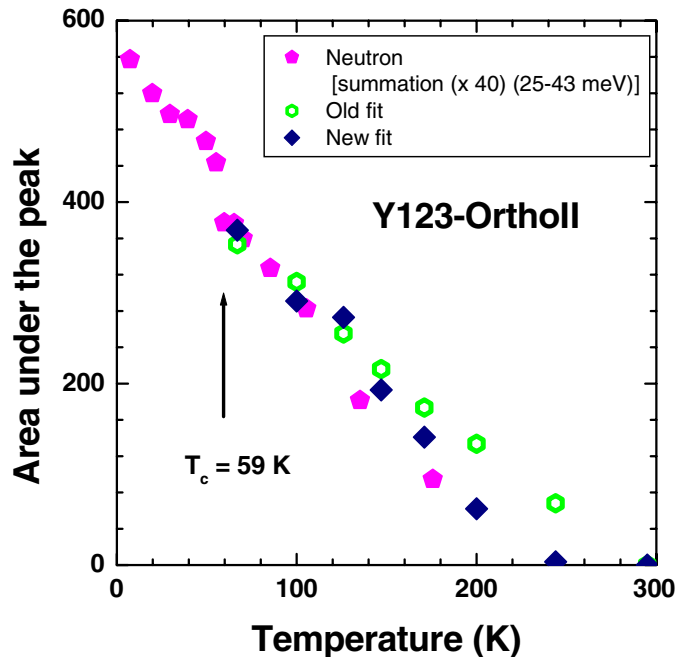


Fig. 3: (Color online) Comparison of the area under the magnetic resonance mode seen in inelastic neutron scattering experiments (solid purple pentagon) [37] and the area under the resonance peak at 31 meV of fig. 2 (solid blue diamond). Also shown are the previous fits of ref. [20] (empty green hexagon) which did not include a recovery region in the electronic density-of-state model.

state at $\omega = 0$ with $\tilde{N}(T, \omega = 0)$ linear in t . A quadratic dependence of $\tilde{N}(T, \omega)$ in ω is assumed till $\omega = \Delta_{pg}$ after which point we have assumed there is a region of increased DOS which contains all the missing states so that by $\omega = 2\Delta_{pg}$ states are conserved. This is a reasonable assumption and certainly supported by our fit for T near T_c . At higher temperatures however, while the data remains consistent with the assumed model, details such as the extent in energy and exact amount of recovery could not be quantitatively pinned down. With this model we calculate the optical scattering time $\tau^{op}(\omega)$ at several temperatures in the normal state with electron-boson spectral density consisting of an MMP background and resonance peak set at 31 meV to agree with the available inelastic neutron scattering data on the local magnetic susceptibility [37]. Two parameters, the amplitude of the background and the area under the resonance peak are varied to get a best least-square fit to the data. The quality of the fit obtained in this way is considerably superior to an earlier fit also based on a pseudogap model but without recovery and Fermi surface arcs. We conclude that the data is more consistent with arcs than without. The effect of the arc shows up clearly in the region just above the main rise in scattering rate where all the curves bunch up together. This is properly captured in our fits while it is missing in the previous analysis. Also our new fits agree better with the neutron studies as to the temperature dependence of

the area under the resonance peak which is one of the important parameter varied in our least-square fit.

This work has been supported by the Natural Science and Engineering Research Council of Canada (NSERC) and the Canadian Institute for Advanced Research (CIAR).

REFERENCES

- [1] TIMUSK T. and STATT B., *Rep. Prog. Phys.*, **62** (1999) 61.
- [2] EMERY V. J. and KIVELSON S. A., *Nature (London)*, **374** (1995) 434.
- [3] CHAKRAVARTY S., LAUGHLIN R. P., MORR D. K. and NAYAK C., *Phys. Rev. B*, **63** (2001) 094503.
- [4] DORA B., VIROSZTEK A. and MAKI K., *Phys. Rev. B*, **65** (2002) 155119; MAKI K., DORA B., KARTSOVNIK M., VIROSZTEK A., KORIN-HAMZIC B. and BASLETIC M., *Phys. Rev. Lett.*, **90** (2003) 256402.
- [5] BENFATTO L. and SHARAPOV S., *Low Temp. Phys.*, **32** (2006) 533.
- [6] ARISTOV D. N. and ZEYHER R., *Phys. Rev. B*, **72** (2005) 115118.
- [7] KIM W. and CARBOTTE J. P., *Phys. Rev. B*, **66** (2002) 033104.
- [8] KIM W., ZHU J. X., CARBOTTE J. P. and TING C. S., *Phys. Rev. B*, **65** (2002) 064502.
- [9] KRASNOV V. M., YURGENS A., WINKLER D., DELSING P. and CLAESON T., *Phys. Rev. Lett.*, **84** (2000) 5960.
- [10] LE TACON M., SACUTO A., GEORGES A., KOTLIAR G., GALLAIS Y., COLSON D. and FORGET A., *Nat. Phys.*, **2** (2006) 537.
- [11] LORAM J. W., MIRZA K. A., COOPER J. R. and TALLON J. L., *J. Phys. Chem. Solids*, **59** (1998) 2091.
- [12] LORAM J. W., LUO J., COOPER J. R., LIANG W. Y. and TALLON J. L., *J. Phys. Chem. Solids*, **62** (2001) 59.
- [13] KANIGEL A., NORMAN M. R., RANDERIA M., CHATTERJEE U., SOUMA S., KAMINSKI A., FRETWELL H. M., ROSENKRANZ S., SHI M., SATO T., TAKAHASHI T., LI Z. Z., RAFFY H., KADOWAKI K., HINKS D., OZYUZER L. and CAMPUZANO J. C., *Nat. Phys.*, **2** (2006) 447.
- [14] HOMES C. C., TIMUSK T., LIANG R., BONN D. A. and HARDY W. V., *Phys. Rev. Lett.*, **71** (1993) 1645.
- [15] HOMES C. C., TIMUSK T., LIANG RUIXING, BONN D. A. and HARDY W. N., *Physica C*, **254** (1995) 265.
- [16] PUCHKOV A. V., BASOV D. N. and TIMUSK T., *J. Phys.: Condens. Matter*, **8** (1996) 10049.
- [17] HWANG J., CARBOTTE J. P. and TIMUSK T., submitted to *Phys. Rev. Lett.* (2007).
- [18] HWANG J., TIMUSK T. and GU G. D., *Nature (London)*, **427** (2004) 714.
- [19] HWANG J., TIMUSK T. and GU G. D., *J. Phys.: Condens. Matter*, **19** (2007) 125208.

- [20] HWANG J., YANG J., TIMUSK T., SHARAPOV S. G., CARBOTTE J. P., BONN D. A., LIANG RUXING and HARDY W. N., *Phys. Rev. B*, **73** (2006) 014508.
- [21] MITROVIC B. and FIORUCCI M. A., *Phys. Rev. B*, **31** (1985) 2694.
- [22] SHARAPOV S. G. and CARBOTTE J. P., *Phys. Rev. B*, **72** (2005) 134506.
- [23] KNIGAVKO A. and CARBOTTE J. P., *Phys. Rev. B*, **72** (2005) 035125.
- [24] KNIGAVKO A. and CARBOTTE J. P., *Phys. Rev. B*, **73** (2006) 125114.
- [25] CARBOTTE J. P., SCHACHINGER E. and HWANG J., *Phys. Rev. B*, **71** (2005) 054506.
- [26] ZASADZINSKI J. F., OZYUZER L., COFFEY L., GRAY K. E., HINKS D. G. and KENDZIORA C., *Phys. Rev. Lett.*, **96** (2006) 017004.
- [27] VALLA T., KIDD T. E., PAN Z.-H., FEDOROV A. V., YIN W.-G., GU G. D. and JOHNSON P. D., cond-mat/0610249 preprint (2006).
- [28] CARBOTTE J. P., SCHACHINGER E. and BASOV D. N., *Nature (London)*, **401** (1999) 354.
- [29] SCHACHINGER E. and CABOTTE J. P., *Phys. Rev. B*, **62** (2000) 9054.
- [30] SCHACHINGER E., NEUBER D. and CARBOTTE J. P., *Phys. Rev. B*, **73** (2006) 184507.
- [31] DORDEVIC S. V., HOMES C. C., TU J. J., VALLA T., STRONGIN M., JOHNSON P. D., GU G. D. and BASOV D. N., *Phys. Rev. B*, **71** (2005) 104529.
- [32] HWANG J., TIMUSK T., SCHACHINGER E. and CARBOTTE J. P., *Phys. Rev. B*, **75** (2007) 144508.
- [33] HWANG J., SCHACHINGER E., CARBOTTE J. P., GAO F., TANNER D. B. and TIMUSK T., cond-mat/0710.4104 preprint (2007).
- [34] SHULGA S. V., DOLGOV O. V. and MAKSIMOV E. G., *Physica C*, **178** (1991) 266.
- [35] ALLEN P. B., *Phys. Rev. B*, **3** (1971) 305.
- [36] MILLIS A. J., MONIEN H. and PINES D., *Phys. Rev. B*, **42** (1990) 167.
- [37] STOCK C., BUYERS W. J. L., COWLEY R. A., CLEGG P. S., COLDEA R., FROST C. D., LIANG R., PEETS D., BONN D., HARDY W. N. and BIRGENEAU R. J., *Phys. Rev. B*, **71** (2005) 024522.